Am J Physiol Heart Circ Physiol 282: H1063–H1070, 2002;
10.1152/ajpheart.00633.2001.

Effects of amiodarone on wave front dynamics during ventricular fibrillation in isolated swine right ventricle

CHIKAYA OMICHI,[1] SHENGMEI ZHOU,[1] MOON-HYOUNG LEE,[1] AJAY NAIK,[1] CHE-MING CHANG,[1] ALAN GARFINKEL,[2] JAMES N. WEISS,[2] SHIEN-FONG LIN,[3] HRAYR S. KARAGUEUZIAN,[1] AND PENG-SHENG CHEN[1]

[1]*Division of Cardiology, Department of Medicine, Cedars-Sinai Medical Center, and* [2]*Division of Cardiology, Departments of Medicine, Physiology, and Physiological Science and the Cardiovascular Research Laboratory, University of California at Los Angeles School of Medicine, Los Angeles, California 90048-1865; and* [3]*Department of Physics and Astronomy, Vanderbilt University, Nashville, Tennessee 37235*

Received 19 July 2001; accepted in final form 12 November 2001

Omichi, Chikaya, Shengmei Zhou, Moon-Hyoung Lee, Ajay Naik, Che-Ming Chang, Alan Garfinkel, James N. Weiss, Shien-Fong Lin, Hrayr S. Karagueuzian, and Peng-Sheng Chen. Effects of amiodarone on wave front dynamics during ventricular fibrillation in isolated swine right ventricle. *Am J Physiol Heart Circ Physiol* 282: H1063–H1070, 2002; 10.1152/ajpheart.00633.2001.—The effects of acute amiodarone infusion on dynamics of ventricular fibrillation (VF) are unclear. Six isolated swine right ventricles (RVs) were studied in vitro. Activation patterns during VF were mapped optically, whereas action potentials were recorded with a glass microelectrode. At baseline, VF was associated with frequent spontaneous wave breaks. Amiodarone (2.5 μg/ml) reduced spontaneous wave breaks and increased the cycle length (CL) of VF from 83.3 ± 17.8 ms at baseline to 118.4 ± 25.8 ms during infusion ($P < 0.05$). Amiodarone increased the reentrant wave front CL (114.4 ± 15.5 vs. 78.2 ± 19.0 ms, $P < 0.05$) and central core area (4.1 ± 3.8 vs. 0.9 ± 0.3 mm^2, $P < 0.05$). Within 30 min of infusion, VF terminated ($n = 1$), converted to ventricular tachycardia (VT) ($n = 1$) or continued at a slower rate ($n = 4$). Amiodarone flattened the APD restitution curves. We conclude that amiodarone reduced spontaneous wave breaks. It might terminate VF or convert VF to VT. These effects were associated with the flattening of APD restitution slope and increased core size of reentrant wave fronts.

optical mapping; action potential duration restitution; sudden death; pharmacology; antiarrhythmic agents

INTRAVENOUS AMIODARONE is a commonly used antiarrhythmic agent in the treatment of life-threatening ventricular tachyarrhythmia (13). However, few studies have examined the mechanisms by which amiodarone is effective against ventricular fibrillation (VF). We (27) previously proposed that transition from ventricular tachycardia (VT) to VF is a transition to spatiotemporal chaos, with similarities to the quasi-periodic route to chaos seen in fluid turbulence. In this scenario, chaos results from the interaction of multiple causally independent oscillatory motions. Computer simulations and animal experiments suggest that the destabilizing oscillatory motions during spiral-wave reentry arise from restitution properties of action potential duration (APD). Modifying APD restitution characteristics can prevent spiral-wave breakup in simulated cardiac tissue, suggesting that drugs with similar effects in real cardiac tissue may have antifibrillatory efficacy (the restitution hypothesis). Intravenous amiodarone is effective in treating patients with life-threatening ventricular arrhythmias and is now included in the new American Heart Association guidelines for advanced cardiopulmonary life support (7). The purpose of this study was to investigate the mechanisms underlying antifibrillatory effects of amiodarone and to determine whether flattening of APD restitution may be involved in its antifibrillatory actions.

METHODS

The research protocol was approved by the institutional animal care and use committee and followed the guidelines of the American Heart Association. The details of the isolated right ventricle (RV) preparation have been reported elsewhere (9). Briefly, six farm pigs (25–32 kg) were anesthetized and the hearts were removed. The RV was placed in tissue bath with the epicardial side up and was perfused with oxygenated Tyrode solution (37.0 ± 0.5°C, pH 7.4 ± 0.5) through the right coronary artery. The composition of the Tyrode solution was the following (in mM): 125.0 NaCl, 4.5 KCl, 0.5 $MgCl_2$, 0.54 $CaCl_2$, 1.2 NaH_2PO_4, 24.0 $NaHCO_3$, 5.5 glucose, and 50 mg/l albumin. Two bipolar electrodes were attached to the epicardial surface: one for continuous recording and the other for pacing. Two Endotak defibrillation electrodes (Guidant) were placed on two opposing sides of the tissue bath for electrical defibrillation.

Optical mapping system. We stained four of six RVs and optically mapped the patterns of epicardial activation. The optical mapping system used in the present study was similar to the one described previously (15). Fluorescence from

Address for reprint requests and other correspondence: P.-S. Chen, Rm. 5342, Cedars-Sinai Medical Center, 8700 Beverly Blvd., Los Angeles, CA 90048-1865 (E-mail: chenp@cshs.org).

The costs of publication of this article were defrayed in part by the payment of page charges. The article must therefore be hereby marked "*advertisement*" in accordance with 18 U.S.C. Section 1734 solely to indicate this fact.

RV epicardium was elicited by a solid state, frequency doubled laser (Verdi, Coherent) at a wavelength of 532 nm. Laser light was delivered to the RV with the use of multiple 1-mm optical fibers (model SP-SF-960, FIS). The RVs were stained for 20 min with 4-[β-2(di-*n*-butylamino)-6-naphthyl]vinyl]pyridinium (di-4-ANEPPS; Molecular Probes) 10 μmol/l in the perfusate. The emitting fluorescence was imaged with a 12-bit digital charge-coupled device camera (model CA-D1–0128T, Dalsa) through a 600-nm long-pass glass filter (model R60, Nikon) and a 25-mm/f0.85 video lens (model CF25L, Fujinon). Video images at 128 × 128 pixels were acquired over 30 × 30 mm^2 at 2.3 ms/frame and were transferred to a personal computer with a frame grabber (Imaging Technology). An excitation-contraction uncoupler was not used in the current study. We recorded 2.3 s of data during each acquisition.

A moving median filter was applied to the optical signal, after which the signals were normalized so that the range of the maximum signal amplitude was the same for each pixel. The signals of each pixel were then spatially averaged. Each pixel was then assigned a shade of gray between white (fully depolarized) and black (fully repolarized). The computer first finds every adjacent pair of pixels in the frame that cross the average value of the data. If the intensity of the data on which the line coincides is increasing, that edge is identified as the wave front and colored red. Otherwise, if it is decreasing, the edge is identified as the wave back and colored green. A point where the red line meets the green line is a wave break (14, 16, 24).

Transmembrane potential recordings and the APD restitution curves. Transmembrane potentials (TMPs) were recorded from an epicardial site using a standard glass microelectrode (9) or pure iridium metal microelectrode (18). For APD measurements, a custom-written program selected as time of activation (*phase 0*) if the voltage change over time (d*V*/d*t*) at that time was greater than both of its temporal neighbors and that the d*V*/d*t* was ≥5 V/s. The program then looked forward in time to determine AP peak (voltage greater than both neighbors) and looked backward in time to determine baseline (voltage less than both neighbors). The voltage difference between the peak and the baseline was the AP amplitude. The program then looked forward in time from the AP peak until the voltage dropped by a value equal to 90% of the AP amplitude. That time is the time of 90% repolarization and the temporal difference between *phase 0* and 90% repolarization is the APD_{90}. The diastolic interval (DI) was defined as the difference between 90% repolarization and the onset of the next activation. Cycle length (CL) was defined by the temporal difference between consecutive activations. Manual editing was then performed to eliminate noise.

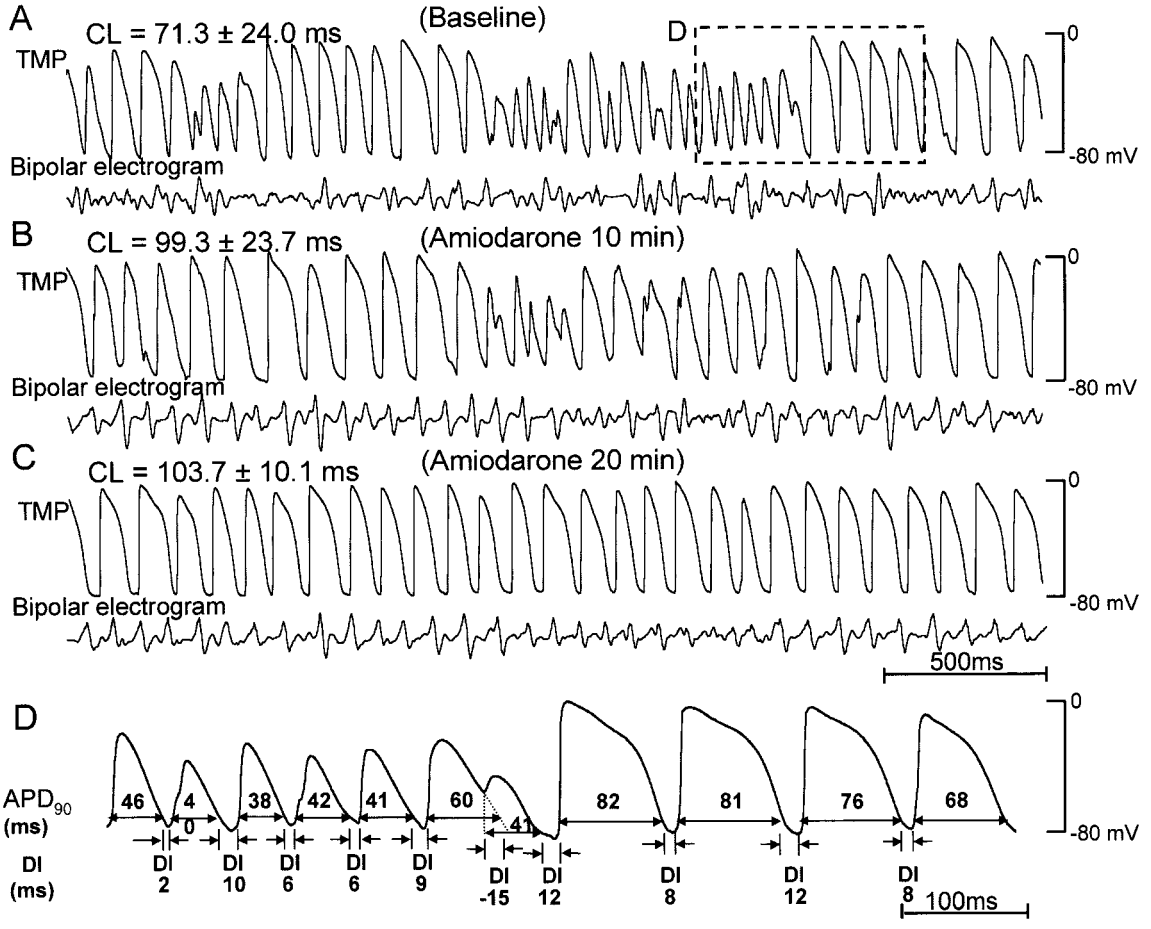

Fig. 1. Transmembrane potentials (TMPs) at baseline (*A*), 10 min (*B*), and 20 min (*C*) after amiodarone infusion. *D*: example of 90% action potential duration (APD_{90}) and difference between 90% repolarization and onset of next activation [diastolic interval (DI)] determination (from area marked by dashed lines in *A*). Note that the cycle length (CL) and APD increased progressively with amiodarone infusion, evolving to a periodic activation resembling ventricular tachycardia (VT).

Figure 1 shows examples of TMP recordings during VF at baseline and after amiodarone infusion (Fig. 1, *A–C*). Figure 1*D* shows an example of TMP analyses. The dashed lines were drawn by manual extrapolation from the action potentials that did not reach 90% repolarization. A "negative DI" (12) can be estimated using the latter method.

We also recorded APD and DI during dynamic pacing (12). This dynamic pacing protocol initially paced the RV at a 400-ms CL at twice the diastolic threshold current for eight beats, followed immediately by eight beats of pacing at 350, 300, 280, 260, 240, 230, 220, 210, 200, 190, 180, 170, and 150 ms CLs.

The APD restitution curve was constructed by plotting APD_{90} against the preceding DI. When DI was ≤ 0, we either omitted those data (first method) or manually estimated the negative DI, as shown in Fig. 1*D* (second method). The APD restitution curve was estimated by single exponential fitting with the use of ORIGIN software (Microcal).

Study protocol. In all isolated RVs, spontaneous VF occurred during the isolation procedure and persisted in the tissue bath. The patterns of activation were mapped while TMPs were simultaneously recorded. Four RVs were defibrillated to allow APD recordings during dynamic pacing. VF was then reinitiated by rapid pacing. Amiodarone (2.5 μg/ml) was then added to the perfusate for 30 min. TMP recordings and optical mapping studies were repeated at 3-min intervals. Reversibility of the effects of amiodarone was assessed with drug-free Tyrode perfusion for 60 min. Inducibility of VF was then tested by electrical stimulation, using the dynamic and fixed rate rapid pacing (CL as short as 50 ms) protocols.

Data analysis. Reentrant wave fronts were identified, and the sizes of their cores were measured by tracing the path of the wave break points. If the path led to a closed loop, then the area encircled by this loop was used as the core size (16). The mean number of wavelets per frame was obtained from the number of wavelets observed every 100 frames (230 ms apart). Density of wavelets was obtained by dividing the number of wavelets by the mapped area (3 cm × 3 cm). The incidence of spontaneous wave breaks was the ratio between the total number of wave breaks observed divided by the total duration of VF analyzed.

Statistical analysis. Data are presented as means ± SD. Student's *t*-tests were used to compare means. Analysis of variance with a Newman-Keuls test was used when multiple comparisons were performed. A P value ≤ 0.05 was considered significant.

RESULTS

Table 1 summarizes the results of the study. At pacing CL of 400 ms, amiodarone significantly decreased the maximum derivative of voltage relation to time [$(dV/dt)_{max}$], prolonged the APD_{90} and increased the effective refractory period (Table 1).

Effects of amiodarone infusion on VF. VF CL, APD_{90}, and DI were prolonged by amiodarone infusion (Table 1). At the end of 30-min infusion, amiodarone resulted in the conversion from VF to VT in 1 RV and VF termination in 1 RV. In the remaining 4 RVs, VF continued at a slower rate. At that time we replaced the perfusate with amiodarone-free Tyrode solution to evaluate the reversibility of the effect of the drug. However, during the drug-free washout period, the VF and VT CLs continued to lengthen and eventually all RVs became quiescent. We then attempted to reinduce VF up to 1 h after the beginning of washout. In no RV was the VF inducible.

Table 1. *Effects of amiodarone*

	Amiodarone, μg/ml		
	Baseline	10 min	20 min
Pacing at 400 ms CL			
$(dV/dt)_{max}$, V/s	40.6 ± 4.9	NA	27.4 ± 2.6*
APD_{90}, ms	194 ± 25	NA	205 ± 14*
Effective refractory period, ms	205 ± 45	NA	238 ± 25*
Dynamic Pacing			
Maximum APD_{90} restitution curve slope by dynamic pacing	2.16 ± 0.44	1.23 ± 0.02	1.20 ± 0.14*
DI at maximum APD_{90} restitution curve, ms	22.0 ± 2.6	30.5 ± 13.4	34.0 ± 9.8
VF			
CL, ms	83.3 ± 17.8	101.3 ± 17.3	118.4 ± 25.8*
APD_{90}, ms	71.1 ± 14.7	77.6 ± 14.6	89.9 ± 19.0*
DI, ms	12.2 ± 9.0	23.7 ± 12.7	28.6 ± 17.0*
Wavelet density, No./cm^2	0.65 ± 0.08	0.47 ± 0.05*	0.41 ± 0.10*
Spontaneous wavebreaks, No./s	35.0 ± 3.4	20.9 ± 2.7*	15.0 ± 2.2*
Reentrant wave front CL, ms	78.2 ± 19.0	96.0 ± 16.4	114.4 ± 15.5*
Core size, mm^2	0.9 ± 0.3	2.5 ± 1.0	4.1 ± 3.8*
Maximum APD_{90} restitution slope during VF	5.24 ± 2.47	3.70 ± 4.40	1.69 ± 1.73*
DI at maximum APD_{90} restitution curve during VF, ms	0.46 ± 0.5	0.8 ± 1.1	0.8 ± 0.3

Values are means ± SD. CL, cycle length; NA, not available; $(dV/dt)_{max}$, maximum derivative of voltage in relation to time; APD_{90}, 90% action potential duration; DI, diastolic interval; VF, ventricular fibrillation. *$P < 0.05$ vs. baseline.

Amiodarone infusion progressively increased CL, reduced the density of wavelets, and the incidence of spontaneous wave breaks (Table 1). Single-cell TMP recordings showed that amiodarone resulted in a reduction of the low amplitude and fast activations in VF, leading to the transition to VT or to a slower CL VF (Fig. 1). We identified 11, 4, and 3 reentrant wave fronts in VF episodes shown in Fig. 1, *A–C*. There was a progressive increase of the CL of reentrant wave front after amiodarone infusion (Table 1).

Video images revealed the effects of amiodarone on wave dynamics during VF. At baseline, VF was characterized by the presence of multiple irregular wave fronts and spontaneous wave breaks (Fig. 2, *top*). These gave rise to the irregular TMP recordings (Fig. 1*A*). Figure 2, *bottom*, illustrates typical activation patterns during amiodarone infusion. A single wave front propagated from the bottom right to the top left corner of Fig. 2. The wavelet propagates repeatedly without breaking, leading in this example to complete elimination of spontaneous wave breaks in the mapped region and a decrease in the number of wavelets. These

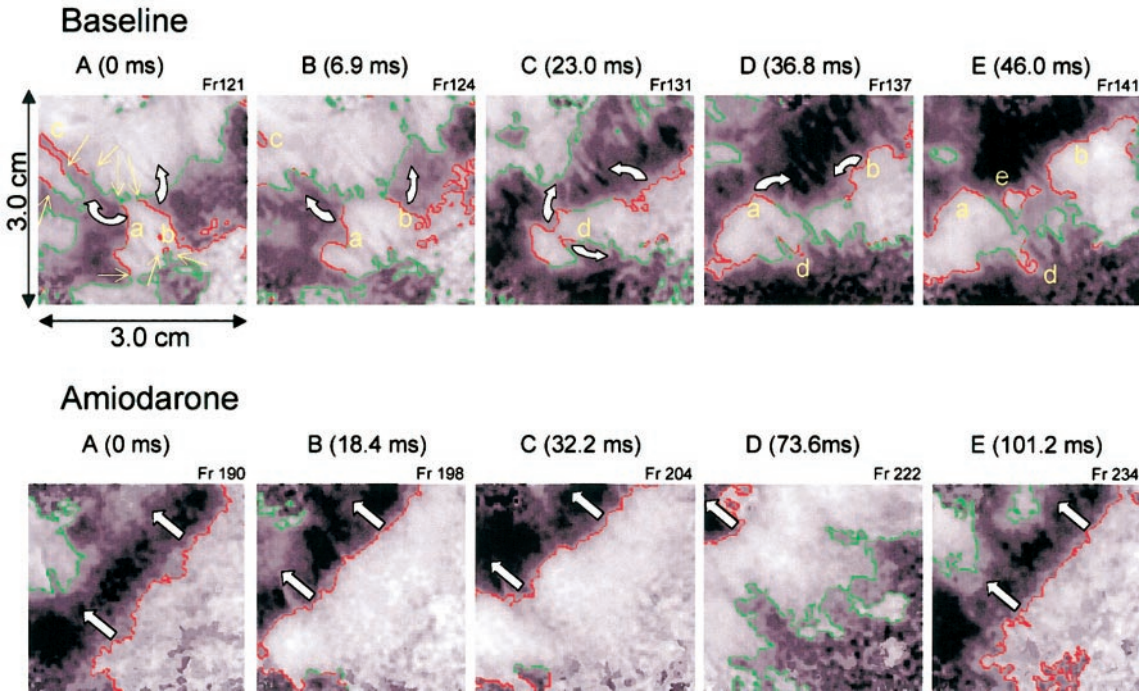

Fig. 2. Activation patterns during ventricular fibrillation (VF) at baseline and during amiodarone infusion. At baseline, 8 wave break points (yellow arrows) are present during the VF. At the time 0 ms, wave fronts marked *a* and *b* are propagating upwards and *wave front c* is propagating to the left outside the mapped area. *Wave front d* in its left portion propagates downward. The new wave front marked *e* breaks up in its central portion, splitting into two wave fronts (*E*, *top*). After amiodarone infusion, a single wave front propagated from the lower right to the top left corner (*A–E*, *bottom*). The wavelet propagates repeatedly without splitting at the site where wave-wave interaction or spontaneous wave breaks occurred at baseline.

changes also gave rise to the periodic activity in the TMP recordings (Fig. 1*C*).

Reentrant wave fronts were occasionally seen during VF at baseline (Fig. 3, *left*). The white arrows indicate counterclockwise reentrant excitation and the tip of the wave front propagates around the central core with a period of 69 ms. The trajectory encircles an area of 0.7 mm^2. During amiodarone infusion, reentrant wave fronts were also observed. Figure 3, *right*, shows a reentrant wave front with a period of 131 ms. A major difference between the reentry circuit at baseline compared with that during amiodarone infusion was the size of the central core around which the wave front rotated (6.8 mm^2). Amiodarone infusion significantly increased the central core area and increased the CL of the reentrant wave fronts (Table 1).

Effects of amiodarone on APD restitution. Figure 4*A* shows action potential recordings at baseline (*left*) and during amiodarone infusion (Fig. 4*A*, *right*). During dynamic pacing, the pacing intervals were fixed for eight beats (S_1), followed by an abrupt shortening of pacing interval. The first beat of the shortened interval is equivalent to a premature stimulus (S_2). This figure shows the AP induced by the last two S_1 and the S_2. The shortest S_1/S_2 achieved at baseline was 160/150 ms, with a corresponding S_2 APD of 113 ms. During amiodarone infusion, the shortest S_1/S_2 increased to 200/190 ms, resulting in an S_2 APD of 148 ms. Figure 4*B* shows an example of dynamic APD restitution curve. Amiodarone increased the APD at all diastolic intervals. Amiodarone significantly reduced the maximum slope of APD_{90} restitution curve. It also appeared to have increased the shortest DI achieved during dynamic pacing. However, the latter increase was not statistically significant (Table 1). Figure 5 shows examples of APD restitution curves during VF at baseline and during amiodarone infusion while RV was still fibrillating. Amiodarone flattened the slope of APD_{90} restitution curve, particularly at short DIs. Table 1 shows the effects of amiodarone infusion in all RVs studied. The DIs associated with the maximum slope of APD_{90} restitution curve at baseline and during amiodarone infusion were $<$10 ms (Table 1).

We also analyzed APD restitution curve by including the negative DI in the graph. However, the APs with negative DIs were $<$1% of the total number of APs analyzed during baseline VF. Adding these negative DIs did not change the restitution curve. For VF after amiodarone infusion, there were fewer (Fig. 1*B*) or no negative DIs recorded.

DISCUSSION

In this study we demonstrated that amiodarone infusion reduced the slope of the APD restitution curve, enlarged the core of reentrant wave front and suppressed spontaneous wave breaks in VF. These changes were associated with a decreased number of

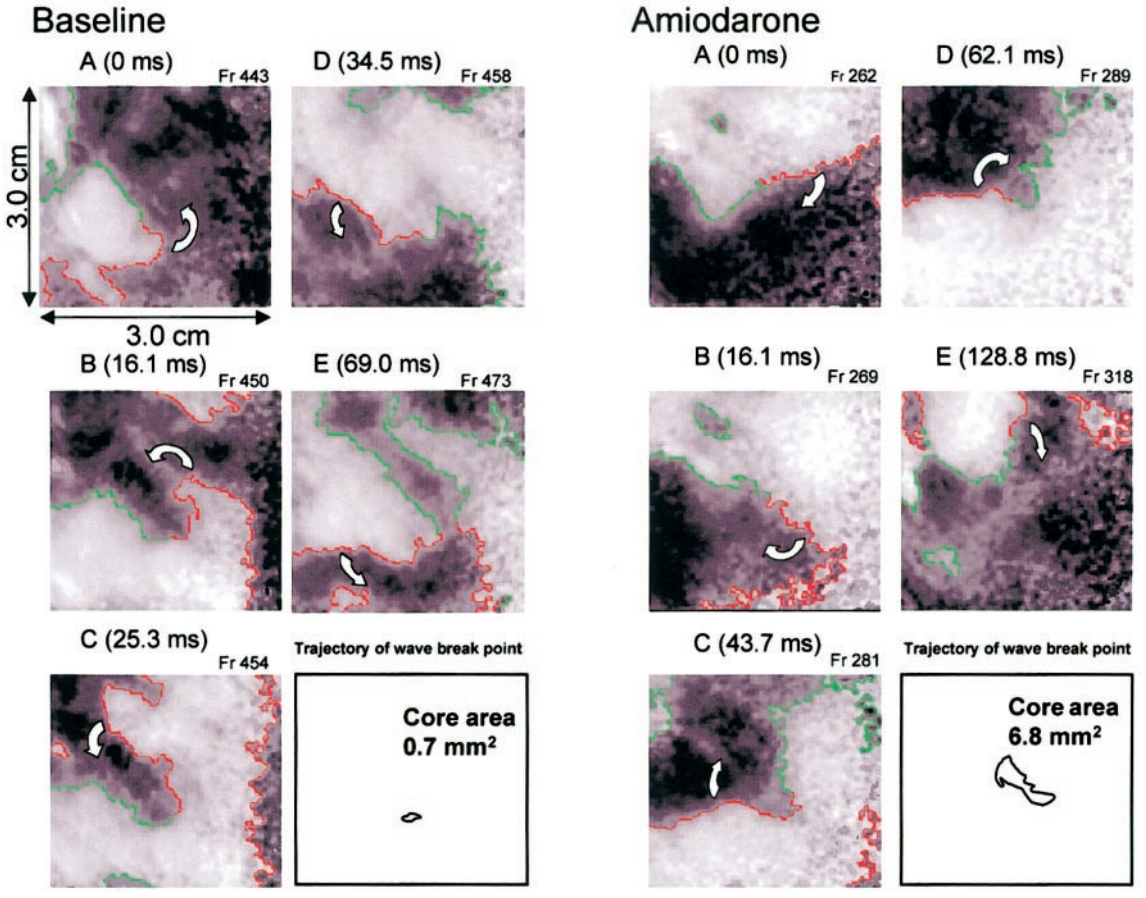

Fig. 3. Reentrant wave front during baseline VF (*left*) and during amiodarone infusion (*right*). A single rotation of the reentrant wave front is displayed at baseline. White arrows indicate counterclockwise reentrant excitation and the wave break point propagates around the central core area. Data are from the same preparation showing one reentrant wave front rotated in a clockwise direction during amiodarone infusion. Note that a major difference between the reentry circuit at baseline compared with that during amiodarone infusion was the central core area around which the front rotated. Amiodarone infusion increased the core area from 0.7 to 6.8 mm^2.

wavelets, the termination of VF, or the transition from VF to VT.

Mechanism of antiarrhythmic drug action. An explanation for the antifibrillatory action of amiodarone is its β-blocking effects (8). Because the RVs were isolated from the rest of the body, they were not influenced by the systemic sympathetic activity. However, local sympathetic nerve terminals might still be active during VF. It is therefore possible that some of the antifibrillatory effects of amiodarone in swine RV were due to β-blocking effects.

A second possible mechanism relates to effects of amiodarone on the CL of the reentrant wave fronts. Recently, Samie et al. (21) proposed that the size and the dynamics of the core of the reentrant wave front, in addition to the effective refractory period, are important determinants of VF. In support of that hypothesis, the authors demonstrated that verapamil increased the size of the core and converted VF to VT in Langendorff-perfused rabbit heart. In the present study, we demonstrate that amiodarone increased the size of the core and reduced the wave front number and spontaneous wave breaks. Therefore, our results are also consistent with the hypothesis proposed by Samie et al. (21).

A third possible mechanism relates to the wavelength hypothesis of cardiac fibrillation (19). Wavelength is a product of refractory period and conduction velocity. Drugs that prolong wavelength are antifibrillatory, whereas drugs that shorten wavelength may be proarrhythmic. Amiodarone and other type III antiarrhythmic agents, such as *d*-sotalol, block the potassium channels (11, 26) and prolong the APD and the refractory period (28). However, amiodarone also blocks the sodium channel (3, 22) and decreases the conduction velocity. A decreased conduction velocity might result in a longer reentrant CL, which could independently lengthen the APD. Furthermore, a uniform reduction of conduction velocity could result in reduced conduction velocity dispersion, a factor that may be associated with improved defibrillation efficacy (23). However, because we mapped only the surface of a three-dimensional RV, we cannot accurately determine the conduction velocity during VF. It cannot be determined in this study whether or not amiodarone alters the wavelength.

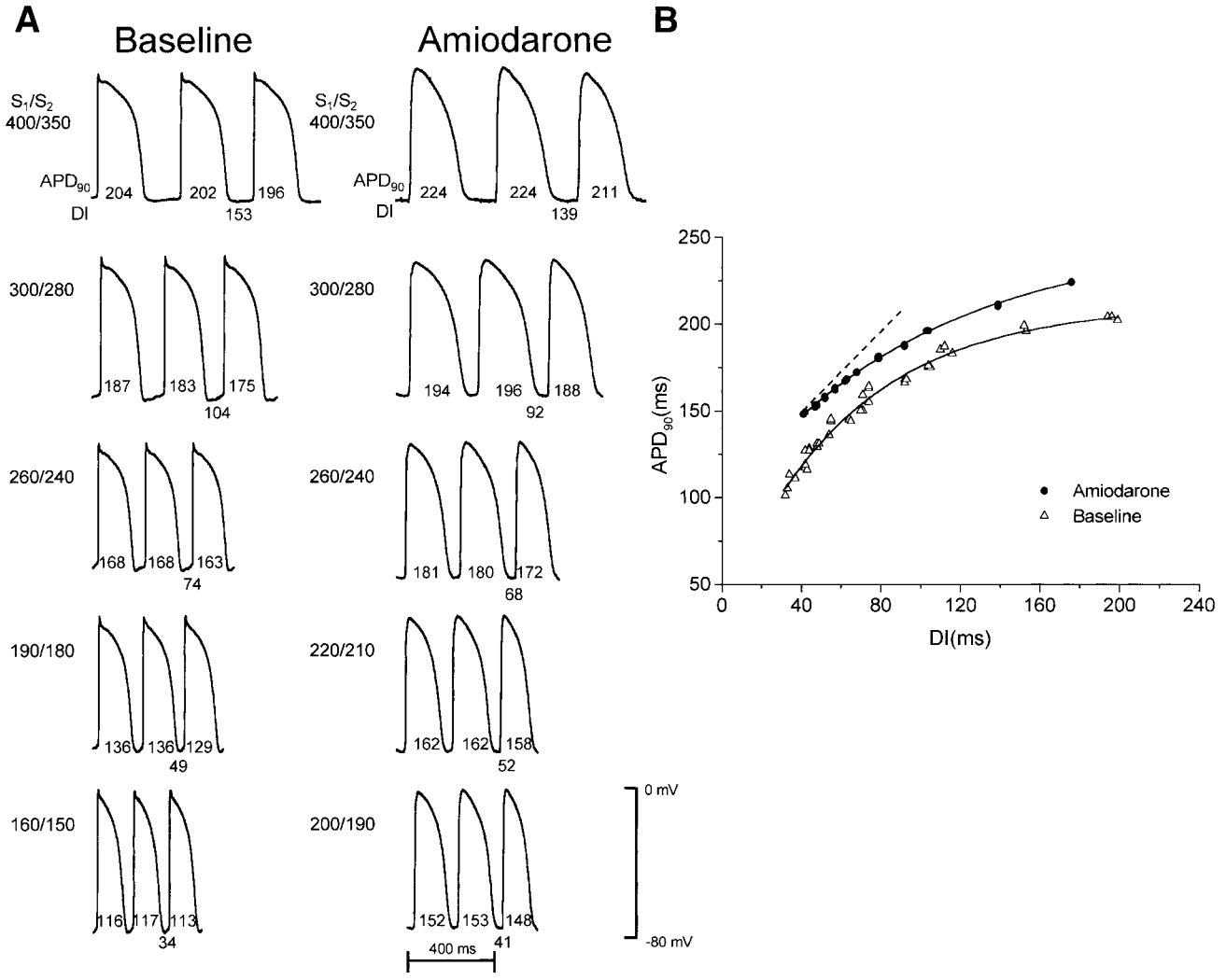

Fig. 4. *A*: APD recordings at baseline and during amiodarone infusion. In each panel, the last 2 paced action potentials and a premature stimulus (S_1 and S_2, respectively), applied at progressively shorter coupling intervals, are shown. *B*: APD restitution curves at baseline and during amiodarone infusion. Note that amiodarone increased the APD at all DIs. A dashed line with a slope of 1 is included for comparison.

A fourth possible explanation is the effect of amiodarone on APD restitution. The restitution hypothesis posits that the APD restitution is a major factors underlying wave break in VF (1, 4, 17, 27). Drugs that flatten the APD restitution curve have antifibrillatory effects (5, 20). A major finding of this study is that amiodarone results in the flattening of the APD restitution slope. This effect could explain the reduced incidence of wave breaks during amiodarone administration. Therefore, our findings are also compatible with the restitution hypothesis.

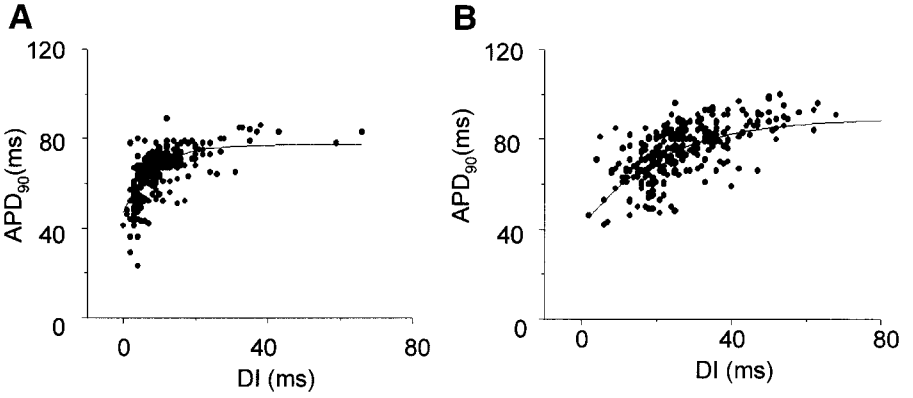

Fig. 5. Examples of APD restitution curve during one episode of VF at baseline (*A*) and one episode 10 min after (*B*) the commencement of amiodarone infusion. Note that amiodarone reduced the slope of the APD restitution curve, particularly at short DIs.

Comparing amiodarone with bretylium and verapamil. Bretylium and verapamil are also effective in flattening the restitution curve (5, 20) but are less useful than amiodarone in treating or preventing clinical VF in human patients. Bretylium (10) results in norepinephrine release during initial administration. It also results in significant orthostatic hypotension and is therefore poorly tolerated. For verapamil to flatten the restitution curve, a concentration of 1,000–3,000 ng/ml is needed (2, 20). This concentration is at least twice as high as what can be achieved with a maximum oral dose of verapamil (120 mg every 6 h) (25). These data indicate that a very high (or toxic) dose of verapamil is needed to reach a serum concentration sufficient to flatten the restitution curve. In comparison, we showed in this study that amiodarone 2.5 μg/ml may flatten restitution curve and exerts significant effects on the patterns of activation in VF. This serum concentration can be easily achieved with 5 mg/kg intravenous amiodarone (6). Therefore, amiodarone is clinically more useful than verapamil or bretylium in treating patients with VT and VF.

Limitation of the study. The first limitation is that acute effects of amiodarone cannot be reversed. Therefore, we were not able to test whether or not the effects of amiodarone are reversible on washout. A second limitation is that we used isolated normal RV in the study. It is unclear whether or not the results are applicable to diseased human hearts. A third limitation is that calcium channel blockers (20) and bretylium (5) are also known to flatten APD restitution. However, these drugs are not as effective as amiodarone in treating human VF. Therefore, flattening of APD restitution may only partially explain the antifibrillatory effects of amiodarone.

In conclusion, amiodarone infusion reduced spontaneous wave breaks and the density of VF wavelets. It might terminate VF or convert VF to VT. These effects were associated with the flattening of APD restitution slope and increased the core size of reentrant wave fronts.

We thank Juliana Cho Glick and Wyeth-Ayerst Laboratories for providing amiodarone used in the study. We also thank Scott Lamp for the data analysis software, Avile McCullen and Meiling Yuan for technical assistance, and Elaine Lebowitz for secretarial assistance.

This study was supported by a grant from Cedars-Sinai Electrocardiographic Heart Beat Organization Foundation and Sweepstakes Award (to H. S. Karagueuzian), a Pauline and Harold Price Endowment (to P.-S. Chen), and the Laubisch and the Kawata Endowments (to J. N. Weiss). This study was also supported in part by National Heart, Lung, and Blood Institute Grants P50-HL-52319 and HL-66389, American Heart Association Grants 9750623N and 9950464N, by University of California Tobacco-Related Disease Research Program Grant 9RT-0041, and by the Ralph M. Parsons Foundation, Los Angeles, CA.

REFERENCES

1. **Cao JM, Qu Z, Kim YH, Wu TJ, Garfinkel A, Weiss JN, Karagueuzian HS, and Chen PS.** Spatiotemporal heterogeneity in the induction of ventricular fibrillation by rapid pacing: importance of cardiac restitution properties. *Circ Res* 84: 1318–1331, 1999.
2. **Colatsky TJ and Hogan PM.** Effects of external calcium, calcium channel-blocking agents, and stimulation frequency on cycle length-dependent changes in canine cardiac action potential duration. *Circ Res* 46: 543–552, 1980.
3. **Follmer CH, Aomine M, Yeh JZ, and Singer DH.** Amiodarone-induced block of sodium current in isolated cardiac cells. *J Pharmacol Exp Ther* 243: 187–194, 1987.
4. **Frame LH and Simson MB.** Oscillations of conduction, action potential duration, and refractoriness. A mechanism for spontaneous termination of reentrant tachycardias. *Circulation* 78: 1277–1287, 1988.
5. **Garfinkel A, Kim YH, Voroshilovsky O, Qu Z, Kil JR, Lee MH, Karagueuzian HS, Weiss JN, and Chen PS.** Preventing ventricular fibrillation by flattening cardiac restitution. *Proc Natl Acad Sci USA* 97: 6061–6066, 2000.
6. **Ikeda N, Nademanee K, Kannan R, and Singh BN.** Electrophysiologic effects of amiodarone: experimental and clinical observation relative to serum and tissue drug concentrations. *Am Heart J* 108: 890–898, 1984.
7. **International Guidelines 2000 for CPR and ECC.** Part 6: advanced cardiovascular life support: section 5: pharmacology I: agents for arrhythmias. *Circulation* 102: I112–I128, 2000.
8. **Kadish AH, Chen RF, Schmaltz S, and Morady F.** Magnitude and time course of β-adrenergic antagonism during oral amiodarone therapy. *J Am Coll Cardiol* 16: 1240–1245, 1990.
9. **Kim YH, Garfinkel A, Ikeda T, Wu TJ, Athill CA, Weiss JN, Karagueuzian HS, and Chen PS.** Spatiotemporal complexity of ventricular fibrillation revealed by tissue mass reduction in isolated swine right ventricle. Further evidence for the quasiperiodic route to chaos hypothesis. *J Clin Invest* 100: 2486–2500, 1997.
10. **Koch-Weser J.** Prevention of sudden coronary death by chronic antiarrhythmic therapy. *Adv Cardiol* 25: 206–228, 1978.
11. **Kodama I, Kamiya K, and Toyama J.** Cellular electropharmacology of amiodarone. *Cardiovasc Res* 35: 13–29, 1997.
12. **Koller ML, Riccio ML, and Gilmour RF Jr.** Dynamic restitution of action potential duration during electrical alternans and ventricular fibrillation. *Am J Physiol Heart Circ Physiol* 275: H1635–H1642, 1998.
13. **Kudenchuk PJ, Cobb LA, Copass MK, Cummins RO, Doherty AM, Fahrenbruch CE, Hallstrom AP, Murray WA, Olsufka M, and Walsh T.** Amiodarone for resuscitation after out-of-hospital cardiac arrest due to ventricular fibrillation. *N Engl J Med* 341: 871–878, 1999.
14. **Lee MH, Lin SF, Ohara T, Omichi C, Okuyama Y, Chudin E, Garfinkel A, Weiss JN, Karagueuzian HS, and Chen PS.** Effects of diacetyl monoxime and cytochalasin D on ventricular fibrillation in swine right ventricles. *Am J Physiol Heart Circ Physiol* 280: H2689–H2696, 2001.
15. **Lin SF, Roth BJ, and Wikswo JP Jr.** Quatrefoil reentry in myocardium: an optical imaging study of the induction mechanism. *J Cardiovasc Electrophysiol* 10: 574–586, 1999.
16. **Mandapati R, Asano Y, Baxter WT, Gray R, Davidenko J, and Jalife J.** Quantification of effects of global ischemia on dynamics of ventricular fibrillation in isolated rabbit heart. *Circulation* 98: 1688–1696, 1998.
17. **Nolasco JB and Dahlen RW.** A graphic method for the study of alternation in cardiac action potentials. *J Appl Physiol* 25: 191–196, 1968.
18. **Omichi C, Lee MH, Ohara T, Naik AM, Wang NC, Karagueuzian HS, and Chen PS.** Comparing cardiac action potentials recorded with metal and glass microelectrodes. *Am J Physiol Heart Circ Physiol* 279: H3113–H3117, 2000.
19. **Rensma PL, Allessie MA, Lammers WJEP, Bonke FIM, and Schalij MJ.** Length of excitation wave and susceptibility to reentrant atrial arrhythmias in normal conscious dogs. *Circ Res* 62: 395–410, 1988.
20. **Riccio ML, Koller ML, and Gilmour RFJ.** Electrical restitution and spatiotemporal organization during ventricular fibrillation. *Circ Res* 84: 955–963, 1999.
21. **Samie FH, Mandapati R, Gray RA, Watanabe Y, Zuur C, Beaumont J, and Jalife J.** A mechanism of transition from ventricular fibrillation to tachycardia: effect of calcium channel

blockade on the dynamics of rotating waves. *Circ Res* 86: 684–691, 2000.
22. **Sheldon RS, Hill RJ, Cannon NJ, and Duff HJ.** Amiodarone: biochemical evidence for binding to a receptor for class I drugs associated with the rat cardiac sodium channel. *Circ Res* 65: 477–482, 1989.
23. **Ujhelyi MR, Sims JJ, and Miller AW.** Induction of electrical heterogeneity impairs ventricular defibrillation: an effect specific to regional conduction velocity slowing. *Circulation* 100: 2534–2540, 1999.
24. **Voroshilovsky O, Qu Z, Lee MH, Ohara T, Fishbein GA, Huang HL, Swerdlow CD, Lin SF, Garfinkel A, Weiss JN, Karagueuzian HS, and Chen PS.** Mechanisms of ventricular fibrillation induction by 60-Hz alternating current in isolated swine right ventricle. *Circulation* 102: 1569–1574, 2000.
25. **Walsh P.** *Physician's Desk Reference*. Montvale, NJ: Medical Economics, 2001, p. 2981.
26. **Wang J, Feng J, and Nattel S.** Class III antiarrhythmic drug action in experimental atrial fibrillation. Differences in reverse use dependence and effectiveness between *d*-sotolol and the new antiarrhythmic drug ambasilide. *Circulation* 90: 2032–2040, 1994.
27. **Weiss JN, Garfinkel A, Karagueuzian HS, Qu Z, and Chen PS.** Chaos and the transition to ventricular fibrillation: a new approach to antiarrhythmic drug evaluation. *Circulation* 99: 2819–2826, 1999.
28. **Yabek SM, Kato R, and Singh BN.** Effects of amiodarone and its metabolite, desethylamiodarone, on the electrophysiologic properties of isolated cardiac muscle. *J Cardiovasc Pharmacol* 8: 197–207, 1986.